ELSEVIER

Biochimica et Biophysica Acta 1512 (2001) 40–52

BIOCHIMICA ET BIOPHYSICA ACTA
BBA

www.bba-direct.com

Bilayer thickness and lipid interface area in unilamellar extruded 1,2-diacylphosphatidylcholine liposomes: a small-angle neutron scattering study

Pavol Balgavý [a,*], Martina Dubničková [a], Norbert Kučerka [a], Mikael A. Kiselev [b], Sergey P. Yaradaikin [b], Daniela Uhríková [a]

[a] *Faculty of Pharmacy, J.A. Comenius University, Odbojárov 10, 832 32 Bratislava, Slovak Republic*
[b] *Frank Laboratory of Neutron Physics, Joint Institute for Nuclear Research, 141980 Dubna, Moscow Region, Russia*

Received 30 October 2000; received in revised form 18 December 2000; accepted 7 January 2001

Abstract

Small-angle neutron scattering (SANS) experiments have been performed on large unilamellar liposomes prepared from 1,2-dilauroylphosphatidylcholine (DLPC), 1,2-dimyristoyl-phosphatidylcholine (DMPC) and 1,2-distearoylphosphatidylcholine (DSPC) in heavy water by extrusion through polycarbonate filters with 500 Å pores. The neutron scattering intensity $I(Q)$ in the region of scattering vectors Q corresponding to $0.0015\ \text{Å}^{-2} \leq Q^2 \leq 0.0115\ \text{Å}^{-2}$ was fitted using a step function model of bilayer neutron scattering length density and supposing that the liposomes are spherical and have a Gaussian distribution of radii. Using the lipid volumetric data, and supposing that the thickness of bilayer polar region equals to $d_H = 9 \pm 1$ Å and the water molecular volume intercalated in the bilayer polar region is the same as in the aqueous bulk aqueous phase, the steric bilayer thickness d_L, the lipid surface area A_L and the number of water molecules per lipid molecule N intercalated in the bilayer polar region were obtained: $d_L = 41.58 \pm 1.93$ Å, $A_L = 57.18 \pm 1.00$ Å^2 and $N = 6.53 \pm 1.93$ in DLPC at 20°C, $d_L = 44.26 \pm 1.42$ Å, $A_L = 60.01 \pm 0.75$ Å^2 and $N = 7.37 \pm 1.94$ in DMPC at 36°C, and $d_L = 49.77 \pm 1.52$ Å, $A_L = 64.78 \pm 0.46$ Å^2 and $N = 8.67 \pm 1.97$ in DSPC at 60°C. After correcting for area thermal expansivity $\alpha \sim 0.00417\ \text{K}^{-1}$, the lipid surface area shows a decrease with the lipid acyl chain length at 60°C: $A_L = 67.56 \pm 1.18$ Å^2 in DLPC, $A_L = 66.33 \pm 0.83$ Å^2 in DMPC and $A_L = 64.78 \pm 0.46$ Å^2 in DSPC. It is also shown that a joint evaluation of SANS and small-angle X-ray scattering on unilamellar liposomes can be used to obtain the value of d_H and the distance of the lipid phosphate group from the bilayer hydrocarbon region d_{H1}.

Keywords: Small-angle neutron scattering; Unilamellar liposome; Bilayer thickness; 1,2-Diacylphosphatidylcholine

1. Introduction

It is well known that the thickness of the lipid bilayer profoundly affects the properties of transmembrane proteins. Textbook examples are the lowering of the stability of open gramicidin A channels caused by the thickness increase [1], the requirement of optimal thickness for maximal activity of (Ca-Mg)ATPase [2] or (Na-K)ATPase [3], and the ion channel blockage under conditions when the bilayer thickness is larger [4] or smaller [5,6] than optimal. The change in the thickness can affect the conforma-

* Corresponding author. Fax: +421-7-5262065;
E-mail: pavol.balgavy@fpharm.uniba.sk

0005-2736/01/$ – see front matter
PII: S0005-2736(01)00298-X

tion [7–9] and/or the lateral aggregation [10,11] of transmembrane proteins. On the other hand, the bilayer can adjust its thickness to match the length of the hydrophobic surface of the protein [12–14]. Determination of the bilayer thickness is thus very important for the characterization of parameters influencing protein–bilayer interactions in membranes.

The simplest method of obtaining bilayer thickness d_L is the evaluation of small-angle X-ray scattering (abbreviation SAXS) or small-angle neutron scattering (abbreviation SANS) on lamellar phases of phospholipids according to Luzzati [15]. It is assumed that the water molecules do not penetrate into phospholipid bilayers. By measuring the relative volumes of water and phospholipid in the sample, one divides the lamellar repeat period, d, into d_L and the thickness of water layer between the bilayers, d_W. The precision and reliability of d_L determination depends on the precision of estimation of the water volume between lamellae. In contrast to the ordered lamellar phase with flat bilayers at low water content, the increase of water content is accompanied by a formation of multilamellar liposomes with curved bilayers and with a large amount of water located not only between the bilayers but also between liposomes [16]. When using the sample content of water for the thickness evaluation, the value obtained is thus flawed [17–20]. The second source of error is the assumption that there are no water molecules located in the bilayer polar region, i.e. that the bilayer is 'dry'. In the second method, the SAXS or SANS on the lamellar phase is evaluated to obtain the electron density profile or the neutron scattering length density profile of the bilayer, respectively [20–24]. In the electron density profile the high intensity peaks correspond to the electron dense phosphate fragments in phospholipid head groups. The head group peak–peak distance across the bilayer, d_{HH}, is then used to calculate the thickness of the bilayer using the known or assumed distance to the outer edge of the bilayer [20,25]. When using the SANS, the obtained neutron scattering length density profiles of deuterium-labeled and protonated phospholipids allow the determination of positions of selectively deuterated phospholipid groups and/or water molecules [26–28].

An alternative way of obtaining the thickness of bilayers is to use unilamellar liposomes. In this case, the SAXS intensity scattering function is Fourier-transformed to obtain the distance distribution function and the bilayer thickness is inferred from it [29–31] or, after inversion of the SAXS scattering function, the thickness is obtained from the position of the first positive non-origin peak in the Patterson function [31,32]. When using the SANS, the bilayer thickness can be obtained from the Kratky–Porod plot of the scattering function in the small range of scattering vectors (see [19,33–40] and references therein), or by fitting the scattering function in a broader range of scattering vectors using a suitable model of the liposomes [41–46].

In the present paper, the thickness of the bilayer in the large extruded unilamellar liposomes from 1,2-diacylphosphatidylcholine with saturated acyl chains (diC_n:0PC, n is the number of carbon atoms in the acyl chain) at temperatures above the gel–fluid phase transition is estimated by using the SANS method. In combination with the volumetric data, the area of lipid at the bilayer–aqueous phase interface is extracted from the SANS data. Finally, the joint evaluation of SANS and SAXS data obtained with unilamellar liposomes is used to determine the distance between the electron dense phosphate fragment and the boundary between the polar and hydrocarbon region of the bilayer.

2. Materials and methods

Synthetic diC12:0PC, diC14:0PC and diC18:0PC were purchased from Avanti Polar Lipids (USA). Heavy water (99.98% ^2H_2O) was obtained from Izotop (Moscow, Russia).

Heavy water and phosphatidylcholine diC_n:0PC were mixed in a glass tube, the tube was purged with pure gaseous nitrogen and sealed with Parafilm M (American National Can, Greenwich, USA) or with a stopper. First, the multilamellar diC_n:0PC liposomes were prepared: The diC_n:0PC in ^2H_2O was dispersed by hand shaking and sonication in a bath sonicator at a temperature above the gel–liquid crystal phase transition temperature of corresponding diC_n:0PC dispersion [47]. From the dispersion of multilamellar liposomes, extruded unilamellar liposomes were prepared according to MacDonald et al. [48] using the LiposoFast Basic extruder (Avestin,

Ottawa, Canada). The multilamellar liposomes were extruded through two polycarbonate filters (Nuclepore, Plesanton, USA) with pores of diameter 500 Å mounted in the extruder fitted with two gas-tight Hamilton syringes (Hamilton, Reno, USA). The sample was subjected to 79 passes through the filters at a temperature above the gel–liquid crystal temperature of the lipid dispersion. An odd number of passes were performed to avoid contamination of the sample by large and multilamellar vesicles, which might not have passed through the filter. The maximum diC*n*:0PC concentration in each sample was 1% (w/w). The samples were flushed with the pure gaseous nitrogen, sealed and stored at room temperature. The maximum period between the sample preparation and its measurement was 3–4 h.

The SANS measurements were performed at the small-angle time-of-flight axially symmetric neutron scattering spectrometer MURN (named now YuMO in honor of deceased Yu. M. Ostanevich) at the IBR-2 fast-pulsed reactor of the Frank Laboratory of Neutron Physics, Joint Institute for Nuclear Research in Dubna [49,50]. The spectrometer is equipped with the circular multiwire proportional ^{3}He detectors [50,51]. The samples were poured into quartz cells (Hellma, Müllheim, Germany) to provide the 2 mm sample thickness. The sample temperature was set and controlled electronically with the precision of ± 0.1°C. The cell with sample was equilibrated for 1 h at the given temperature in the sample holder before measurement. The scattering patterns were corrected for background effects and the neutron scattering cross section was obtained by using a vanadium standard scatterer as described in [50].

3. Results and discussion

3.1. Experimental data

Fig. 1 shows the plot of the typical experimental SANS scattering curve, $I(Q)$, of unilamellar liposomes as a function of the scattering vector Q which is defined as:

$$Q = 4\pi\sin\theta/\lambda \quad (1)$$

where 2θ is the scattering angle and λ the wavelength of neutrons. It is seen from the Fig. 1 that the relative accuracy of $I(Q)$ values is decreased at larger Q values. This is due to reduction of SANS with the increase of the scattering angle. The neutron scattering intensity per unit neutron flux on the sample and per unit volume for a monodisperse system can be written as:

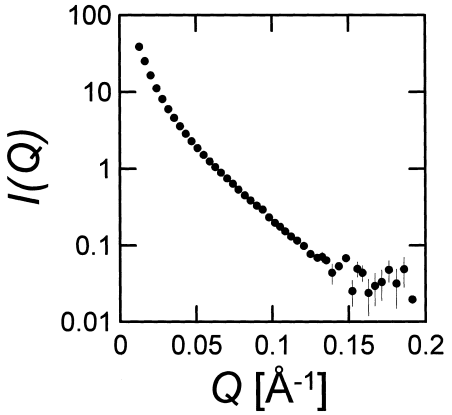

Fig. 1. The dependence of SANS intensity $I(Q)$ on scattering vector for extruded unilamellar diC12:0PC liposomes. The dots indicate the mean values obtained by averaging over seven circular detectors and the error bars the standard error of the mean value.

$$I(Q) = N_P P(Q) S(Q) \quad (2)$$

where N_P is the number of particles, $P(Q)$ is the particle structure factor and $S(Q)$ is the size- and orientation-dependent interparticle structure factor which depends on the number of particles and ion–ion and dipole–dipole interactions between their surfaces [52]. It has been found experimentally, that at the PC concentration in the sample as used in the present study (1% w/w) $S(Q) \cong 1$ [33,34,53,54], and deviations occur at concentrations $\geq 2\%$ (w/w) (M.A. Kiselev, P. Lesieur, A.M. Kisselev, D. Lombardo, in preparation, see also [54,55]).

3.2. Kratky–Porod analysis of experimental data

In analogy to the scattering on planar two-dimensional sheet which thickness is small in comparison to its lateral dimensions [52,56], several groups of authors [19,33,34,37,38,54,57,58] have supposed that in the small range of scattering vectors the scattering intensity for unilamellar liposomes dispersed in

heavy water can be written as:

$$I(Q) = I(0)Q^{-2}\exp(-Q^2R_g^2) \quad (3)$$

where $I(0)$ and R_g are constants. The value of R_g is obtained from the Kratky–Porod plot of data ($\ln[I(Q)Q^2]$ vs. Q^2). From the value of R_g, the bilayer thickness parameter d_g can be obtained [33] as:

$$d_g^2 = 12R_g^2 \quad (4)$$

A typical Kratky–Porod plot of experimental SANS data is shown in Fig. 2. It is seen that the data can be fitted well by a linear function up to $Q^2 = 0.02$ Å^2. At higher values of Q, deviations from the linearity as well as larger scatter of data are observed. A closer inspection of the data in the smallest region of scattering vectors has shown, that the curve is non-linear also for $Q^2 < 0.001$ Å^{-2}. After a careful inspection of all measured data, we have selected the region of 0.0015 Å$^{-2} \leq Q^2 \leq 0.0115$ Å^{-2} for fitting of experimental curves. The values of R_g and thickness parameters d_g thus obtained are listed in Table 1. These data can be compared with the SAXS results of Lewis and Engelman [32] obtained with sonicated unilamellar phosphatidylcholine liposomes. They have evaluated the transbilayer distance between electron dense phosphate groups d_{HH} from the Patterson function analysis. Since the Patterson inversion of scattering data was done in a limited region of Q values, their values of d_{HH} were underestimated due to systematic truncation errors. Nagle and Tristram-Nagle [20] have estimated recently that the actual d_{HH} is larger for about 1.0 Å than the original values in [32]. The correct d_{HH} values are listed in Table 1. We have included in this table also the available data for unilamellar egg yolk phosphatidylcholine (EYPC) liposomes. The R_g and d_g values were obtained from our experimental SANS data published in [19] but recalculated in the present work using the 0.0015 Å$^{-2} \leq Q^2 \leq 0.0115$ Å^{-2} region. The d_{HH} value for EYPC liposomes is from the paper of Wilkins et al. [59] who found 35 Å from the Patterson function. We have corrected this by adding 1 Å because of truncation error. Fig. 3 shows the plot of d_{HH} as a function of d_g thickness parameter. It is seen that the d_{HH} and d_g values correlate (linear correlation, $r^2 = 0.997$). This correlation indicates that the thickness parameter d_g reflects rather well changes in the bilayer thickness.

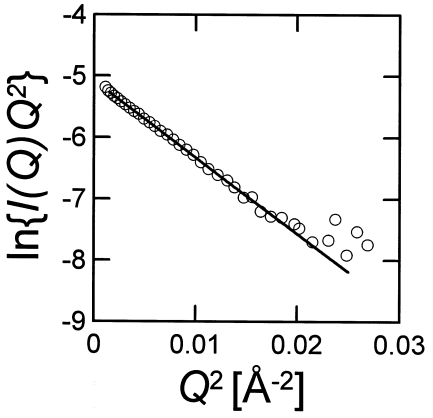

Fig. 2. Kratky–Porod plot of experimental SANS curve for extruded unilamellar diC14:0PC liposomes.

Table 1
'Gyration radius' R_g, bilayer thickness parameter d_g, steric bilayer thickness d_L, surface area A_L, bilayer polar region thickness d_H and number N of water molecules intercalated in the polar region of extruded unilamellar diCn:0PC liposomes

	T (°C)	R_g^2 (Å^2)	d_g (Å)	d_L (Å)	A_L (Å^2)	N	d_{HH} (Å)	d_{HH} (Å)	A_L (Å^2) at 60°C, $\alpha = 0.003$ K^{-1}	A_L (Å^2) at 60°C, $\alpha = 0.00417$ K^{-1}
diC10:0PC	20						26.5$^{\#}$	27.5§		
diC12:0PC	20	108.70 ± 1.51	36.12 ± 0.25	41.58 ± 1.93	57.18 ± 1.00	6.53 ± 1.93	30.5$^{\#}$	31.5§	64.47 ± 1.13*	67.56 ± 1.18*
diC14:0PC	36	124.20 ± 0.90	38.61 ± 0.14	44.26 ± 1.42	60.01 ± 0.75	7.37 ± 1.94	34.0$^{\#}$	35.0§	64.49 ± 0.81*	66.33 ± 0.83*
diC16:0PC	44						37.0$^{\#}$	38.0§		
diC18:0PC	60	163.54 ± 0.81	44.30 ± 0.11	49.77 ± 1.52	64.78 ± 0.46	8.67 ± 1.97	40.5$^{\#}$	41.5§	64.78 ± 0.46	64.78 ± 0.46
EYPC	20	130.75 ± 0.59	39.61 ± 0.09				35.0$^{\#}$	36.0§		

For comparison, the bilayer thickness parameter d_{HH} obtained from SAXS data of sonicated diCn:0PC [32] and EYPC [59] liposomes ($^{\#}$) and corrected for truncation errors (§) by Nagle and Tristram-Nagle [20] are shown. The values marked by * were obtained by using the thermal expansion adjustment (Eq. 10) to the A_L data.

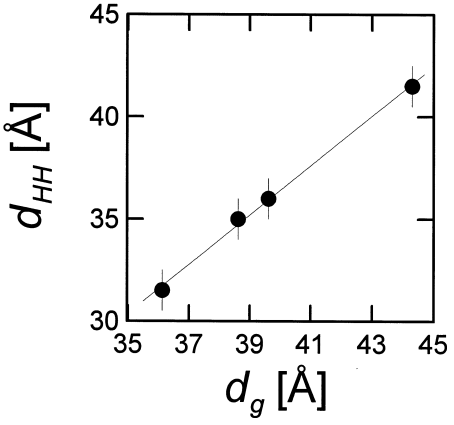

Fig. 3. Correlation of bilayer thickness parameters d_g and d_{HH}.

Furthermore, the correlation between d_{HH} and d_g could be used to obtain the bilayer structural parameters from the d_g data via the known relations between them and d_{HH}.

While the d_{HH} parameter obtained from the Patterson function and corrected for the truncation error can be ascribed to the transbilayer distance of the electron dense phosphate groups, the molecular interpretation of the d_g thickness parameter is not so straightforward. We have simulated the SANS on phosphatidylcholine liposomes in our recent papers [19,40] using a model of polydisperse hollow spheres. When these spheres are dispersed in heavy water without any water molecules located in their bilayer, then the value of d_g obtained by using Eqs. 3 and 4 is close to the thickness of such 'dry' bilayer. Experimentally, we found in [19] that d_g obtained from SANS data of unilamellar EYPC liposomes is equal within experimental error to the bilayer thickness estimated from the X-ray diffraction data of fully hydrated fluid lamellar EYPC phase using Luzzati's model of diffraction data evaluation [15]. However, this model is rather crude and far from reality because some amount of water is located in the polar region of the bilayer. In the following we thus develop a more realistic model for the SANS data interpretation.

3.3. Multishell model of polydisperse liposomes

We suppose that unilamellar liposomes are spherical. For the centrosymmetrical particles, the particle structure factor $P(Q)$ is equal to the square of form factor, which is the one-dimensional Fourier integral of the scattering length density:

$$F(Q) = -4\pi \int_0^\infty r^2 \rho(r) \frac{\sin(Qr)}{Qr} \mathrm{d}r \tag{5}$$

where the integration is over the whole space [52]. We suppose further, that each of the two monolayers in the bilayer in unilamellar liposomes consists of two shells. The polar head group shell containing the phospholipid polar head groups and some fixed number of water molecules N per phospholipid is characterized by the thickness d_H and the non-polar hydrocarbon shell consisting of methylene and methyl groups of acyl chains is characterized by the thickness d_C. The steric bilayer thickness is then:

$$d_L = 2d_H + 2d_C \tag{6}$$

We finally suppose, that the neutron scattering length density (ρ_i), different for each shell of the bilayer, is homogeneous within each shell. The Fourier integral is thus divided into the integrals over the bilayer shells. Then the scattering intensity without the background can be calculated using equations:

$$I(Q) = N_P \left(\frac{4\pi}{Q^3}\right)^2 \left\{ \sum_i \Delta\rho_i (A_{i+1} - A_i \right\}^2;$$

$$A_i = Q\, a_i \cos(Q\, a_i) - \sin(Q\, a_i) \tag{7}$$

where $\Delta\rho_i = \rho_w - \rho_i$ are the contrast values of neutron scattering length densities against aqueous phase (ρ_w) for the individual shells, and a_i are borders of the shells. These equations are valid for a monodisperse system. However, experimentally prepared unilamellar liposomes have some degree of polydispersity [48,60–63] which can be described by different distribution functions. For example, in the previous SANS studies of unilamellar EYPC liposomes, Gaussian [19,40,41] and Schultzian [42,45,60,64] size distributions were used. In the range of Q values used below, the particular distribution has practically no effect on results obtained (Kučerka et al., unpublished, see also [46,64]). In the present paper, we use for simplicity the Gaussian distribution in the form:

$$f(R_2) = \frac{1}{\sqrt{2\pi}\sigma_R} \exp\left[-\frac{(R_2 - R_{2,\mathrm{mean}})^2}{2\sigma_R^2} \right] \tag{8}$$

where R_2 is the outer liposome radius, $R_{2,mean}$ is the mean outer radius of liposomes, and the polydispersity of liposome sizes is expressed by σ_R.

The neutron scattering intensity of model spherical polydisperse liposomes can be thus computer-simulated by summing over all individual intensities obtained from Eq. 7, and convoluted by the distribution function (Eq. 8) and the spectrometer resolution function [50]. The convolution by the distribution function smears totally the fast $I(Q)$ oscillations dependent on the liposome radius [19,40,45].

3.4. Simulation of scattering curves

As an illustration of the Kratky–Porod plot of simulated data, Figs. 4 and 5 show the results for diC16:0PC in ^2H_2O at 50°C. In these simulations, we have used the values of neutron coherent scattering length densities of atoms published in [65], the volume of the diCn:0PC polar head group (including glycerols and carbonyls) $V_H = 319$ Å^3 [66,67] and of the diC16:0PC hydrophobic region $V_C = V_L - V_H = 913$ Å^3 where $V_L = 1232$ Å^3 is the diC16:0PC molecular volume estimated experimentally at 50°C [68,69]. The volume of each ^2H_2O molecule located in the polar shell $V_{^2H_2O} = 30.338$ Å^3 was the same as observed in bulk ^2H_2O at 50°C [70], i.e. we supposed that the partial specific volume of water located in the bilayer is the same as in the bulk aqueous phase. Experimental findings support this assumption

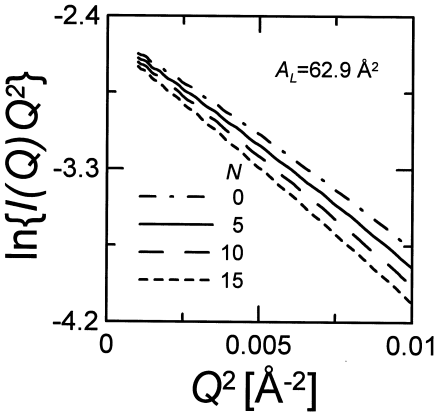

Fig. 4. Kratky–Porod plots of simulated SANS curves for the constant value of lipid area $A_L = 62.9$ Å^2 and different numbers N of water molecules located in the bilayer polar region. Data were obtained for diC16:0PC liposomes ($R_{2,mean} = 300$ Å, $\sigma_R = 91$ Å) in ^2H_2O.

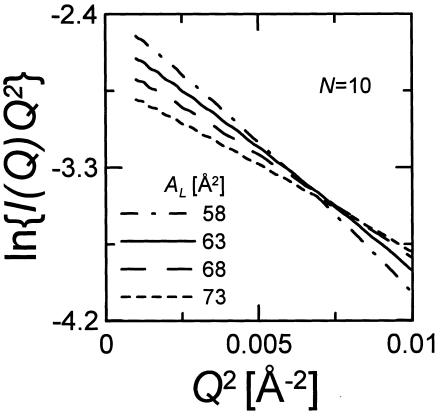

Fig. 5. Kratky–Porod plots of simulated SANS curves for the constant number $N = 10$ of water molecules located in the bilayer polar region and different values of lipid area A_L. Data were obtained for diC16:0PC liposomes ($R_{2,mean} = 300$ Å, $\sigma_R = 91$ Å) in ^2H_2O.

[19,71]. In the distribution function (Eq. 8), we have used a parabolic relation between the mean outer liposome radius and σ_R found in our previous paper [19]. To illustrate the effect of water intercalation into the polar region on the scattering function, we have fixed the value of diC16:0PC surface area on the bilayer–aqueous phase interface to the constant $A_L = 62.9$ Å^2 and varied the number of water molecules N (Fig. 4), and vice versa (Fig. 5). It is seen that each simulated curve can be approximated by a linear function in the region of Q^2 values shown. In the selected range of Q values, we have also observed that the value of mean liposome radius typical of extruded liposomes (200 Å $\leq R_{2,mean} \leq$ 500 Å) has no effect on the slope of this linear function for each combination of the bilayer thickness d_L (or the lipid surface area A_L) and the number of water molecules $0 \leq N \leq 20$ intercalated into the bilayer polar region studied. In analogy to the scattering on a planar two-dimensional sheet which thickness is small in comparison to its lateral dimensions, the root of absolute value of this slope is frequently named gyration radius R_g. However, it should be clear that the value of R_g is not equal to the gyration radius of lipid bilayer – it is just a measure of the slope of linear function approximating the $\ln[I(Q)Q^2]$ vs. Q^2 curve in the selected Q^2 range. We should like also to stress that the value of R_g is dependent on the selection of this Q^2 range. Furthermore, it is seen from the simulated data in Figs. 4

and 5 that this slope is sensitive to both the number N of intercalated water molecules in the bilayer polar region and to the surface area A_L (or the bilayer thickness d_L).

3.5. Evaluation of experimental data using the multishell model of polydisperse liposomes

The procedure of the evaluation of experimental data using the multishell model of liposomes is simple. In the first step the value of N is fixed. For this fixed N, the value of $\ln[I(Q)Q^2]$ is calculated at some starting value of d_L (or A_L) for those Q^2 values in the interval $0.0015\ \text{Å}^{-2} \leq Q^2 \leq 0.0115\ \text{Å}^{-2}$ where the experimental data were taken. From this simulated curve, the value of R_g(sim) is obtained by fitting the simulated data and compared with the experimental R_g value obtained in the same interval. Then the value of d_L (or A_L) is changed stepwise until $|R_g - R_g(\text{sim})| \leq 0.001$ Å. The result is the d_L and A_L values for the given N. The value of N is then changed and the whole procedure repeated again and again to obtain other N, d_L and A_L combinations.

To calculate the contrast values of neutron scattering length densities $\Delta\rho_i = \rho_w - \rho_i$ against aqueous phase for the individual shells, the volumes of these shells must be guessed or known from independent volumetric experiments. The volumetric parameters used in the evaluation of the experimental data are collected in Table 2. The molecular volumes V_L of diC14:0PC, diC16:0PC and diC18:0PC were obtained from the absolute specific volumes v_L (estimated by a combination of neutral buoyancy method and differential dilatometry in [72]) as:

$$V_L = v_L M_w / N_A \quad (9)$$

where M_w is the phosphatidylcholine molecular weight and N_A the Avogadro number. To obtain the hydrocarbon region volume V_C (i.e. the sum of volumes of methyl and methylene groups of the lipid acyl chains), the volume of the head group $V_H = 319$ Å^3 [66,67,73] was subtracted from the molecular volume V_L. It is supposed that the head group volume is not influenced by the temperature and the acyl chain length of the lipid. Because of the absence of experimental volumetric data for diC12:0PC and diC10:0PC, the procedure was different. The temperature dependencies of experimental values of V_C in the fluid phases of diC14:0PC, diC16:0PC and diC18:0PC were extrapolated to 20°C. Then these extrapolated values were plotted as a function of acyl chain length and extrapolated again to obtain the V_C value for diC12:0PC. Using this procedure, we have found $V_C = 674$ Å^3 and $V_L = V_H + V_C = 993$ Å^3. Using Eq. 9, we have obtained then $v_L = 0.962$ ml/g for diC12:0PC at 20°C from the value of V_L. Cornell and Separovic [74] used the value of $v_L = 0.9627$ ml/g for diC12:0PC 'at temperature 20°C above the phase transition' which is -1.75 ± 0.02°C according to [47]. Supposing that the volume of acyl chain methyl group $V_3 = 1.9 V_2$ where V_2 is the volume of acyl chain methylene group [67], one gets $V_2 = 28.32$ Å^3 and $V_3 = 53.81$ Å^3 for diC12:0PC at 20°C. A similar procedure gave $V_C = 561$ Å^3 and $V_L = 880$ Å^3 for diC10:0PC at 20°C. The volume of the water molecule located in the head group region was supposed to be the same as in the bulk aqueous phase and the volumetric data collected for heavy water in [70] were used.

The fitting procedure described above gives the values of A_L, d_L, d_H and d_C as a function of N. As an example of the obtained results, Fig. 6 demonstrates the dependence of A_L on N for diC18:0PC. Because of an experimental error in the R_g value, the values obtained by the fitting procedure are bound by two curves and the possible values of A_L lie between these curves. Similar curves have been obtained for the dependencies of d_L, d_H and d_C on N for all diC_n:0PC liposomes studied (not shown).

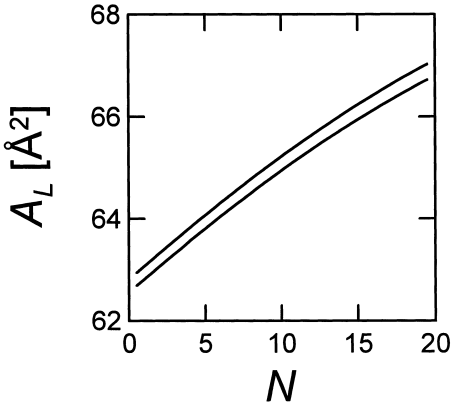

Fig. 6. Dependence of the lipid surface area A_L on the number of water molecules N intercalated in the polar region of extruded diC18:0PC liposomes at 60°C.

These results can now be used for comparisons with the results of other authors. To make these comparisons comfortable for readers of the present paper, we have approximated our results for A_L and d_L by polynomials and collected them in Table 3. We have included in this table also the values of uncertainties ΔA_L and Δd_L propagating from the experimental errors in R_g values. As an example, we compare now our data for diC14:0PC with selected data from the literature. Koenig et al. [18] have obtained the value of $A_L = 59.5 \pm 0.2$ Å^2 extrapolated to zero osmotic pressure from X-ray diffractograms of the fluid diC14:0PC lamellar phase measured at different osmotic pressures at 30°C and evaluated according to Luzzati [15]. Petrache et al. [66] have found from the electron density profiles in the fully hydrated diC14:0PC bilayers in the lamellar fluid phase at 30°C that the number of water molecules penetrated into the bilayer polar region is $N = 7.3$, the lipid surface area $A_L = 59.7 \pm 0.2$ Å^2 and the steric bilayer thickness $d_L = 44.2$ Å. This is very close to the steric bilayer thickness $d_L = 44.0$ Å in unilamellar diC14:0PC liposomes obtained from their SAXS curves by Laggner et al. [29] at 28°C. Using the value of $N = 7.3$, one calculates from our SANS data $A_L = 60.08 \pm 0.23$ Å^2 and $d_L = 44.21 \pm 0.19$ Å at 36°C. Using the area thermal expansivity:

$$\alpha = \frac{1}{A_L}\left(\frac{\partial A_L}{\partial T}\right)_\pi \quad (10)$$

where T is the absolute temperature and $\alpha \approx T0.00417 \pm 0.00020$ K^{-1} at 34°C [75,76], one obtains finally from our data $A_L = 58.59 \pm 0.30$ Å^2 at 30°C. Nagle and Tristram-Nagle [20] corrected the data from [18] and [66] and obtained $A_L = 59.5$ Å^2 and $N = 7.2$, and $A_L = 59.6$ Å^2 and $d_L = 44.2$ Å, respectively. From this new value of N one calculates from our data $A_L = 60.04 \pm 0.23$ Å^2 and $d_L = 44.14 \pm 0.19$ Å at 36°C or $A_L = 58.55 \pm 0.30$ Å^2 at 30°C. Nagle and Tristram-Nagle [20] have used $\alpha \sim 0.003$ K^{-1} for bilayers in the fluid state at temperatures far from the gel–fluid phase transition temperature. When using this value of α, one obtains $A_L = 58.99 \pm 0.25$ Å^2 for $N = 7.2$–7.3 and at 30°C from our data. The agreement between our results and the results in papers [18,20,29,66] is excellent. The values $A_L = 55.8 \pm 0.6$ Å^2 and $d_L = 40.7 \pm 0.4$ Å obtained by Lemmich et al. [22] for the fluid lamellar phase of perdeuterated diC14:0PC at 28.5°C seem to be underestimated. Similar comparisons can be done for other diCn:0PC liposomes studied and other literature data.

In the SAXS studies, the bilayer polar region thickness d_H is frequently set to some constant value known from independent experiments or calculations to obtain the bilayer thickness from electron density profile (see [20] for references). This constrain can be used also in the SANS data evaluation and it is possible then to obtain all three parameters N, A_L and d_L from SANS data simultaneously. Simply, from the dependencies of A_L, d_L, d_H and d_C on N obtained from SANS data as described above, only those combinations are selected where the polar region thickness is equal to the known or supposed d_H value. The thickness of the polar region d_H can be deduced from the data of other authors. Pabst et al. [24] extracted $d_H = 9.0 \pm 1.2$ Å from the neutron diffraction data of oriented and partially hydrated diC16:0PC bilayers published in [27,28]. McIntosh and Simon [77] estimated $d_H = 10$ Å from space-filling models of PC. Nagle et al. [69] used $d_H = 8$ Å for fluid diC16:0PC bilayers and Petrache et al. [73] $d_H = 9$ Å for fluid diC14:0PC and EYPC bilayers. We have used in our calculations $d_H = 9.0 \pm 1.0$ Å which covers practically all the literature data. We have obtained then the values of N, A_L and d_L sum-

Table 2
Volumetric data for phosphatidylcholine bilayers

	diC10:0PC	diC12:0PC	diC14:0PC	diC16:0PC	diC18:0PC
T (°C)	20	20	36	44	60
v_L (ml/g)	0.937	0.962	0.984	1.0025	1.028
V_L (Å^3)	880	993	1108	1222	1348
V_H (Å^3)	319	319	319	319	319
V_C (Å^3)	561	674	789	903	1029
$V_{^2H_2O}$ (Å^3)	30.073	30.073	30.185	30.281	30.480

marized in Table 1. The uncertainties given for these values propagate from the experimental errors of R_g and from the uncertainty in d_H. Especially in the case of diC14:0PC, our results are very close to the N, A_L and d_L values obtained from SAXS data in [18,20,29,66]. There is also good agreement between our value of $N = 7.37 \pm 1.94$ and the values of $N = 9.7 \pm 0.5$ and $N = 8.6 \pm 1.9$ estimated in the fluid diC14:0PC bilayers by solid state NMR spectroscopy [78] and radiolabel centrifugal technique [79], respectively.

The estimated lipid surface area A_L increases with the increase of the lipid acyl chain length (see Table 1), but this is mainly caused by the fact that the temperature at which the samples were measured increased in the same direction. The increased temperature increases the probability of *gauche* rotamers formation in acyl chains [80] and this results in the increased lipid surface area. To compare the values of A_L at the same temperature, we have applied the thermal expansion adjustment (Eq. 10) to these data. When using the thermal expansivity $\alpha = 0.003$ K^{-1}, the ranges of lipid surface area for diC12:0PC, diC14:0 and diC18:0PC overlap at 60°C (Table 1). However, when higher value $\alpha = 0.00417$ K^{-1} is used, then the obtained data indicate a decrease in A_L with the increase of acyl chain length at this temperature (Table 1). Morrow et al. [81] have observed using ^{2}H NMR spectroscopy of fully hydrated chain perdeuterated diCn:0PC multilamellar liposomes that the inverse acyl chain extension per acyl chain segment along the bilayer normal (which is proportional to the lipid surface area) increases with the acyl chain length at temperatures where all studied lipids (acyl chain lengths $n = 12$, 14, 16, 18) are in the fluid phase, including at 60°C. Combining this with our results, one can conclude that more reliable results are those obtained with higher α value. The decrease of A_L with n can be expected – the van der Waals attraction between the acyl chains should increase with the acyl chain length, and this decreases the lipid surface area.

It should be noted that the d_H values used above were obtained in lamellar phases of PCs, where the phosphocholine group of diCn:0PC orients predominantly parallel to the bilayer plane. However, the phosphocholine group can rotate from this position and orient perpendicularly to the bilayer plane extending about 2–3 Å farther into the aqueous phase. This might occur more frequently in unilamellar liposomes [82,83]. The value of d_H used in evaluation of data obtained with unilamellar liposomes must be therefore checked in another way. We have done this by a joint evaluation of SAXS and SANS data.

3.6. Simultaneous evaluation of SANS and SAXS data

In the simultaneous evaluation of the SAXS and SANS data the distance between the phosphate group and the boundary between the polar and hydrocarbon region of the bilayer:

$$d_{H1} = (d_{HH} - 2d_C)/2 \quad (11)$$

is needed. Lewis and Engelman [32] estimated $d_{H1} = 5.5$ Å from the neutron diffraction data obtained with oriented and partially hydrated PC bilayers in [27,28]. Nagle and Tristram-Nagle (chapter 10.1 in [20]) concluded from the molecular dynamics simulations of fluid phase diC16:0PC bilayer [67] that the molecular tilt and conformational disorder reduces this value to about $d_{H1} = 5.2$ Å. They have used this latter value of d_{H1} to obtain the surface area of diC14:0PC and diC16:0PC from the SAXS d_{HH} values obtained in unilamellar liposomes (see chapter 10.1 and table 5 in [20]). The same group of authors used $d_{H1} = 4.1$ Å for getting the surface areas from the d_{HH} values obtained in fluid lamellar phases of diC14:0PC and EYPC [73]. Later, Nagle and Tristram-Nagle [20] have concluded that this latter value was too small and have used $d_{H1} = 4.9$ Å for bilayers in fluid lamellar phases of diC14:0PC, diC16:0PC, EYPC and dioleoylphosphatidylcholine (see chapter 13 and table 6 in [20]). When trying to evaluate simultaneously the SANS and the SAXS data obtained with unilamellar liposomes for the all diCn:0PC liposomes studied, we have found that different d_{H1} values had to be used for liposomes prepared from different diCn:0PC lipids. Our procedure of joint SANS and SAXS data evaluation was simple. First, the distance d_{H1} was set to some fixed value from the interval 4.1 Å $\leq d_{H1} \leq$ 5.5 Å and the surface area was calculated as:

$$A_L = 2V_C/(d_{HH} - 2d_{H1}) \quad (12)$$

Table 3
Dependencies of A_L and d_L on N obtained from SANS data

Lipid	$A_L = a+bN+cN^2$				$d_L = d+eN+fN^2$			
	a (Å^2)	b (Å^2)	c (Å^2)	ΔA_L (Å^2)	d (Å)	e (Å)	f (Å)	Δd_L (Å)
diC12:0PC	53.990	0.498	−0.00129	0.45	36.806	0.762	−0.00445	0.29
diC14:0PC	57.246	0.402	−0.00197	0.23	38.727	0.772	−0.00278	0.19
diC18:0PC	62.685	0.265	−0.00256	0.15	43.021	0.783	−0.00053	0.13

where d_{HH} and V_C used were from Tables 1 and 2, respectively. Using this surface area, the number of water molecules N intercalated in the bilayer polar region was obtained from the dependencies of A_L on N like in Fig. 6 or in Table 3. Then the polar region thickness was obtained as:

$$d_H = (V_L + NV_W - V_C)/A_L \quad (13)$$

where V_L, V_C and V_W used were from Table 2. In the following cycles, other d_{H1} values were used to obtain other sets of A_L, N and d_H values. The rows in the matrix of (d_{H1} N A_L d_H) values that did not fulfil rather weak constrains 8 Å $\leq d_H \leq$ 12 Å or $5 \leq N \leq 12$ were then excluded. The ranges of obtained values of d_{H1} and d_H are shown in Table 4. It is seen that the spread of obtained distances between the phosphate group and the boundary between the polar and hydrocarbon region of the bilayer is closer to the lower limit of d_{H1} interval taken into account in case of short chain lipids (diC12:0PC and diC14:0PC), while it is closer to the higher limit in case of long chain lipid (diC18:0PC). This might indicate that this part of bilayer polar region is more conformationally disordered in short chain lipids. The spread in the obtained d_H values is $\leq$3 Å for each lipid and there is a tendency of the decrease in d_H with the increase in lipid acyl chain length. This might be another indication of lower conformational disorder in the polar region of diC18:0PC bilayers. The higher limit of obtained d_H values for diC12:0PC and diC14:0PC (but not for diC18:0PC) bilayers in unilamellar liposomes is larger than that in the fluid lamellar phases discussed above. This might indicate higher probability of phosphocholine group rotation in the position perpendicular to the bilayer plane. The ranges of allowed number of water molecules N obtained were rather broad but never reached the constrained limits.

The estimated lipid surface area A_L increases with the increase of the lipid acyl chain length (see Table 4 and Fig. 7, symbols ♦), but this is caused by the temperature effect as discussed above. When using the thermal expansivity $\alpha = 0.00417$ K^{-1}, the ranges of lipid surface area for diC12:0PC, diC14:0 and diC18:0PC obtained from the joint SANS and SAXS data indicate a decrease in A_L with the increase of acyl chain length at 60°C (Table 4 and Fig. 7, symbols ×). This trend is more expressive when the A_L value of C10:0PC unilamellar liposomes evaluated from the SAXS data is taken into

Table 4
The diCn:0PC bilayer structural data

Lipid	T (°C)	d_{H1} (Å)	A_L (Å^2)	N	d_H (Å)	A_L (Å^2) at 60°C, $\alpha = 0.00417$ K^{-1}
diC10:0PC	20	4.10–4.50[#]	58.14–60.65			68.69–71.66
diC12:0PC	20	4.10–4.47[§]	57.85–59.75	7.927–11.997	9.63–11.37	68.36–70.60
diC14:0PC	36	4.19–4.73[§]	59.281–61.78	5.141–11.987	8.00–11.00	65.52–68.29
	30	4.9*	59.6*	7.2*	9*	67.54
diC16:0PC	44	4.20–4.70[#]	61.01–63.15			65.22–67.50
	44	4.90–5.20[#]	64.04–65.44			68.46–69.95
	44	4.6[#]	62.71			67.03
	50	4.9*	64*	8.6*	9*	66.72
diC18:0PC	60	5.22–5.43[§]	66.26–67.17	6.943–11.981	8.01–10.19	66.26–67.17

The distance of the phosphate group from the bilayer hydrocarbon region d_{H1} was obtained by simultaneous evaluation of SAXS and SANS data ([§]) or guessed ([#]). The values marked by * were obtained from [20].

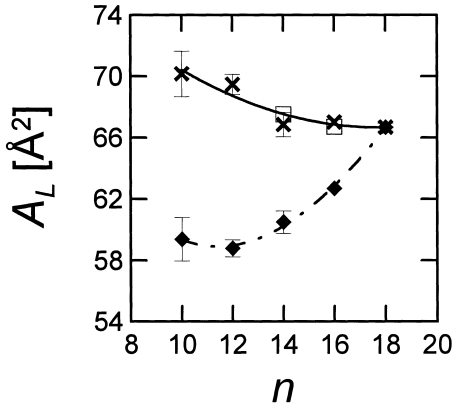

Fig. 7. Dependence of the lipid surface area A_L on the number of carbon atoms n in the diCn:0PC acyl chain. (♦) Values obtained at temperatures shown in Table 1, (×) values extrapolated to 60°C by using $\alpha = 0.00417$ K^{-1}, (□) values obtained from the data of Nagle and Tristram-Nagle [20]. The values × at $n = 16$ were obtained by using $d_{H1} = 4.6$ Å.

account. To do this, we have supposed that the distance between the phosphate group and the boundary between the polar and hydrocarbon region in these liposomes is close to that found in diC12:0PC and diC14:0PC liposomes. The range of A_L values thus obtained from the SAXS d_{HH} value and extrapolated to 60°C by using thermal expansivity $\alpha = 0.00417$ K^{-1} is rather large, nevertheless it fits into a decreasing tendency of A_L with the acyl chain length. We have included in Table 4 and Fig. 7 also the data for fully hydrated fluid lamellar phases of diC14:0PC and diC16:0PC published in [20]. After extrapolation to 60°C, these data fit well to our dependencies of A_L on acyl chain length (Fig. 7, symbols □). In Table 4 and Fig. 7, shows also a very good agreement between our A_L results obtained from the joint evaluation of SAXS and SANS data of diC14:0PC unilamellar liposomes and that published by Nagle and Tristram-Nagle in [20] for the fluid lamellar phase of diC14:0PC. However, we have obtained $d_{H1} = 4.19$–4.73 Å for this lipid in unilamellar liposomes, while Nagle and Tristram-Nagle [20] used $d_{H1} = 4.9$ Å in the fluid lamellar phase. This result could indicate that the lipid surface area is the same both in the unilamellar liposomes and in the lamellar phase, though the conformation disorder in the polar part of the bilayer might be slightly different in these systems. This conclusion is further supported by the comparison of diC16:0PC data (see Table 4). The best agreement between the A_L values extrapolated to 60°C has been obtained supposing $d_{H1} = 4.6$ Å in unilamellar liposomes, while the data of lamellar phase were obtained using $d_{H1} = 4.9$ Å. It is also seen from Table 4 that small changes in d_{H1} bring about relatively large changes in the extrapolated values of A_L.

The precision of the results obtained from the simultaneous evaluation of SANS and SAXS would be higher when more precise SAXS were available. The SAXS experiments have one disadvantage – the low contrast between phospholipid bilayer and the aqueous phase. In the case of unilamellar liposomes, sucrose solutions can sufficiently increase the contrast without influence on the bilayer thickness [84–86]. In future studies SANS and SAXS data obtained with liposomes suspended in aqueous sucrose solution and evaluated as shown in the present paper could provide a very detailed picture of the lipid bilayer.

4. Conclusions

We have shown that the SANS on extruded unilamellar phosphatidylcholine liposomes dispersed in heavy water provides data that can be used in combination with the volumetric data to obtain the steric bilayer thickness, the lipid surface area at the bilayer–aqueous phase interface, and the number of water molecules intercalated in the bilayer polar region. We have also shown how the joint evaluation of SANS and SAXS on unilamellar liposomes can be used to obtain thicknesses of the bilayer polar and hydrophobic regions, and the distance between the phosphate group and the boundary between the polar and hydrocarbon region of the bilayer. We have used a rather simple step function model of bilayer neutron scattering length density in combination with experimental volumetric data. An obvious extension of this model would be a model with diffuse steps of scattering length densities to simulate fluctuations in the bilayer thickness and in positions of lipid groups. An important extension would be a non-homogeneous distribution of water molecules in the bilayer polar region. Also deviations of the liposome shapes from the spherical symmetry and non-Gaussian distributions of liposome sizes could be taken into account. This work is in progress in our group.

Acknowledgements

M. Dubničková, N. Kučerka and D. Uhríková thank the staff of the Condensed Matter Division, Frank Laboratory of Neutron Physics, Joint Institute for Nuclear Research in Dubna, Russia for hospitality, M. Kiselev thanks the Laboratory of Biophysics, Department of Physical Chemistry, Faculty of Pharmacy, Comenius University in Bratislava, Slovakia, for the financial support and hospitality. The authors thank Prof. John F. Nagle and Dr. Klaus Gawrisch for critical reading of the manuscript of this paper and Dr. Nathan Janes and Dr. Barbara Frisken for comments. This study was supported by the Slovak Ministry of Education grant to P. Balgavý and by the J.A. Comenius University grant to N. Kučerka. The experiments in Dubna were supported within the Project 07-4-1031-99/03 'Investigation of the structure and dynamics of condensed matter with neutrons'.

References

[1] D.A. Haydon, S.B. Hladky, Q. Rev. Biophys. 5 (1972) 187–282.
[2] A. Johannsson, C.A. Keightley, G.A. Smith, C.D. Richards, T.R. Hesketh, J.C. Metcalfe, J. Biol. Chem. 256 (1981) 1643–1650.
[3] A. Johannsson, G.A. Smith, J.C. Metcalfe, Biochim. Biophys. Acta 641 (1981) 416–421.
[4] D.A. Haydon, B.M. Hendry, S.R. Levinson, J. Requena, Nature 268 (1977) 356–358.
[5] B.M. Hendry, J.R. Elliott, D.A. Haydon, Biophys. J. 47 (1985) 841–845.
[6] M.S. Braun, D.A. Haydon, Pflüg. Arch. 418 (1991) 62–67.
[7] A.P. Starling, J.M. East, A.G. Lee, Biochem. J. 310 (1995) 875–879.
[8] A.P. Starling, J.M. East, A.G. Lee, Biochem. J. 308 (1995) 343–346.
[9] A.G. Lee, Biochim. Biophys. Acta 1376 (1998) 381–390.
[10] B.A. Lewis, D.M. Engelman, J. Mol. Biol. 166 (1983) 203–210.
[11] R.L. Cornea, D.D. Thomas, Biochemistry 33 (1994) 2912–2920.
[12] K. He, S.J. Ludtke, W.T. Heller, H.W. Huang, Biophys. J. 71 (1996) 2669–2679.
[13] Y. Kobayashi, K. Fukada, Biochim. Biophys. Acta 1371 (1998) 363–370.
[14] T.A. Harroun, W.T. Heller, T.M. Weiss, L. Yang, H.W. Huang, Biophys. J. 76 (1999) 937–945.
[15] V. Luzzati, in: D. Chapman (Ed.), Biological Membranes, Academic Press, London, 1968, pp. 71–124.
[16] K. Gawrisch, W. Richter, A. Möpps, P. Balgavý, K. Arnold, G. Klose, Stud. Biophys. 108 (1985) 5–16.
[17] G. Klose, B. König, H.W. Meyer, G. Schulze, G. Degovics, Chem. Phys. Lipids 47 (1988) 225–234.
[18] B.W. Koenig, H.H. Strey, K. Gawrisch, Biophys. J. 73 (1997) 1954–1966.
[19] P. Balgavý, M. Dubničková, D. Uhríková, S. Yaradaikin, M. Kiselev, V. Gordeliy, Acta Phys. Slovaca 48 (1998) 509–533.
[20] J.F. Nagle, S. Tristram-Nagle, Biochim. Biophys. Acta 1469 (2000) 159–195.
[21] V.I. Gordeliy, M.A. Kiselev, Biophys. J. 69 (1995) 1424–1428.
[22] J. Lemmich, K. Mortensen, J.H. Ipsen, T. Honger, R. Bauer, O.G. Mouritsen, Phys. Rev. E 53 (1996) 5169–5180.
[23] R. Zhang, S. Tristram-Nagle, W. Sun, R.L. Headrick, T.C. Irving, R.M. Suter, J.F. Nagle, Biophys. J. 70 (1996) 349–357.
[24] G. Pabst, M. Rappolt, H. Amenitsch, P. Laggner, Phys. Rev. E 62 (2000) 4000–4009.
[25] T.J. McIntosh, S.A. Simon, Biochemistry 25 (1986) 4058–4066.
[26] G. Büldt, H.U. Gally, A. Seelig, J. Seelig, G. Zaccai, Nature 271 (1978) 182–184.
[27] G. Büldt, H.U. Gally, J. Seelig, G. Zaccai, J. Mol. Biol. 134 (1979) 673–691.
[28] G. Zaccai, G. Büldt, A. Seelig, J. Seelig, J. Mol. Biol. 134 (1979) 693–706.
[29] P. Laggner, A.M. Gotto Jr., J.D. Morrisett, Biochemistry 18 (1979) 164–171.
[30] P. Laggner, K. Lohner, G. Degovics, K. Müller, A. Schuster, Chem. Phys. Lipids 44 (1987) 31–60.
[31] P.R. Maulik, D. Atkinson, G.G. Shipley, Biophys. J. 50 (1986) 1071–1077.
[32] B.A. Lewis, D.M. Engelman, J. Mol. Biol. 166 (1983) 211–217.
[33] W. Knoll, J. Haas, H.B. Stuhrmann, H.H. Füldner, H. Vogel, E. Sackmann, J. Appl. Crystallogr. 14 (1981) 191–202.
[34] V.I. Gordeliy, L.V. Golubchikova, A. Kuklin, A.G. Syrykh, A. Watts, Prog. Colloid Polym. Sci. 93 (1993) 252–257.
[35] S.N. Shashkov, M.A. Kiselev, S.N. Tioutiounnikov, A.M. Kisselev, P. Lesieur, Physica B 271 (1999) 184–191.
[36] M.A. Kiselev, P. Lesieur, A.M. Kisselev, C. Grabiel-Madelmond, M. Ollivon, J. Alloys Compd. 286 (1999) 195–202.
[37] T. Gutberlet, M. Kiselev, H. Heerklotz, G. Klose, Physica B 276–278 (2000) 381–383.
[38] D. Uhríková, P. Balgavý, N. Kučerka, A. Islamov, V. Gordeliy, A. Kuklin, Biophys. Chem. 88 (2000) 165–170.
[39] M.A. Kiselev, P. Lesieur, D. Lombardo, A.M. Kisselev, T. Gutberlet, Chem. Phys. Lipids 107 (2000) 72.
[40] P. Balgavý, N. Kučerka, V.I. Gordeliy, V.G. Cherezov, Acta Phys. Slovaca 51 (2001) 53–68.
[41] S. Komura, Y. Toyoshima, T. Takeda, Jpn. J. Appl. Phys. 21 (1982) 1370–1372.

[42] J.S. Pedersen, S.U. Egelhaaf, P. Schurtenberger, J. Phys. Chem. 99 (1995) 1299–1305.
[43] R.J. Gilbert, R.K. Heenan, P.A. Timmins, N.A. Gingles, T.J. Mitchell, A.J. Rowe, J. Rossjohn, M.W. Parker, P.W. Andrew, O. Byron, J. Mol. Biol. 293 (1999) 1145–1160.
[44] P.C. Mason, B.D. Gaulin, R.M. Epand, G.D. Wignall, J.S. Lin, Phys. Rev. E 59 (1999) 3361–3366.
[45] J. Pencer, F.R. Hallet, Phys. Rev. E 61 (2000) 3003–3008.
[46] H. Schmiedel, P. Joerchel, M.A. Kiselev, G. Klose, J. Phys. Chem. B 105 (2001) 111–117.
[47] G. Lipka, B.Z. Chowdhry, J.M. Sturtevant, J. Phys. Chem. 88 (1984) 5401–5406.
[48] R.C. MacDonald, R.I. MacDonald, B.P. Menco, K. Takeshita, N.K. Subbarao, L.R. Hu, Biochim. Biophys. Acta 1061 (1991) 297–303.
[49] V.A. Vagov, A.B. Kunchenko, Yu.M. Ostanevich, I.M. Salamatin, JINR Commun. P14 83 (1983) 898.
[50] Yu.M. Ostanevich, Macromol. Chem. Macromol. Symp. 15 (1988) 91–103.
[51] B.N. Ananyev, A.B. Kunchenko, V.I. Lazin, E.Ya. Pikelner, JINR Commun. 3 (1978) 11502.
[52] L.A. Feigin, D.I. Svergun, Structure Analysis by Small-Angle X-Ray and Neutron Scattering, Plenum, New York, 1987.
[53] A.G. Muddle, J.S. Higgins, P.G. Cummins, E.J. Staples, I.A. Lyle, Faraday Discuss. Chem. Soc. 76 (1983) 77–92.
[54] T. Nawroth, H. Conrad, K. Dose, Physica B 156/157 (1989) 477–480.
[55] M.A. Kiselev, P. Lesieur, D. Lombardo, A.M. Kisselev, M. Ollivon, Chem. Phys. Lipids 107 (2000) 72–73.
[56] O. Kratky, P. Laggner, in: Encyclopedia of Physical Science, Vol. 14, Academic Press, London, 1987, pp. 693–742.
[57] V.I. Gordeliy, V.G. Cherezov, J. Teixeira, J. Mol. Struct. 383 (1996) 117–124.
[58] M. Dubničková, M. Kiselev, S. Kutuzov, F. Devínsky, V. Gordeliy, P. Balgavý, Gen. Physiol. Biophys. 16 (1997) 175–188.
[59] M.H. Wilkins, A.E. Blaurock, D.M. Engelman, Nat. New Biol. 230 (1971) 72–76.
[60] F.R. Hallet, B. Nickel, C. Samuels, P.H. Krygsman, J. Electron Microsc. Tech. 17 (1991) 459–465.
[61] H. Hauser, in: G. Cevc (Ed.), Phospholipids Handbook, M. Dekker, New York, 1993, pp. 603–637.
[62] D.G. Hunter, B.J. Frisken, Biophys. J. 74 (1998) 2996–3002.
[63] A.J. Jin, D. Huster, K. Gawrisch, R. Nossal, Eur. Biophys. J. 28 (1999) 187–199.
[64] M.A. Kiselev, P. Lesieur, A.M. Kisselev, D. Lombardo, M. Killany, S. Lesieur, J. Alloys Compd., in press.
[65] V.F. Sears, Neutron News 3 (1992) 29–37.
[66] W.J. Sun, R.M. Suter, M.A. Knewtson, C.R. Worthington, S.T. Nagle, R. Zhang, J.F. Nagle, Phys. Rev. E 49 (1994) 4665–4676.
[67] H.I. Petrache, S.E. Feller, J.F. Nagle, Biophys. J. 72 (1997) 2237–2242.
[68] J.F. Nagle, M.C. Wiener, Biochim. Biophys. Acta 942 (1988) 1–10.
[69] J.F. Nagle, R. Zhang, S. Tristram-Nagle, W. Sun, H.I. Petrache, R.M. Suter, Biophys. J. 70 (1996) 1419–1431.
[70] Handbook of Chemistry and Physics, The Chemical Rubber Co., Cleveland, OH, 1969.
[71] M.C. Wiener, S. Tristram-Nagle, D.A. Wilkinson, L.E. Campbell, J.F. Nagle, Biochim. Biophys. Acta 938 (1988) 135–142.
[72] J.F. Nagle, D.A. Wilkinson, Biophys. J. 23 (1978) 159–175.
[73] H.I. Petrache, S. Tristram-Nagle, J.F. Nagle, Chem. Phys. Lipids 95 (1998) 83–94.
[74] B.A. Cornell, F. Separovic, Biochim. Biophys. Acta 733 (1983) 189–193.
[75] E. Evans, D. Needham, J. Phys. Chem. 55 (1987) 309–313.
[76] D. Needham, E. Evans, Biochemistry 27 (1988) 8261–8269.
[77] T.J. McIntosh, S.A. Simon, Biochemistry 25 (1986) 4948–4952.
[78] C. Faure, L. Bonakdar, E.J. Dufourc, FEBS Lett. 405 (1997) 263–266.
[79] S. Channareddy, S.S. Jose, N. Janes, J. Am. Chem. Soc. 119 (1997) 2345–2347.
[80] J. Gallová, Ph.D. thesis, Faculty of Mathematics and Physics, J.A. Comenius University, Bratislava, 1993.
[81] M.R. Morrow, J.P. Whitehead, D. Lu, Biophys. J. 63 (1992) 18–27.
[82] H. Hauser, M.C. Phillips, B.A. Levine, R.J.P. Williams, Nature 261 (1976) 390–394.
[83] H. Hauser, Biochim. Biophys. Acta 646 (1981) 203–210.
[84] M.A. Kiselev, P. Lesieur, JINR Commun. D9 102 (2000) 120–126.
[85] P. Lesieur, M.A. Kiselev, L.I. Barsukov, D. Lombardo, J. Appl. Crystallogr. 33 (2000) 623–627.
[86] M.A. Kiselev, P. Lesieur, A.M. Kisselev, D. Lombardo, M. Killany, S. Lesieur, M. Ollivon, Nucl. Instrum. Methods, in press.